

## Chemistry of the Phosphorus–Nitrogen Ligands. Multiple Isomeric Transformations of the Diphosphinohydrazine Bearing 8-Quinolyl Substituent: P→C, P→N, and P→P Migrations Caused by Different Factors

Alexander N. Kornev,\* Natalia V. Belina, Vyacheslav V. Sushev, Julia S. Panova, Olga V. Lukoyanova, Sergey Y. Ketkov, Georgy K. Fukin, Mikhail A. Lopatin, and Gleb A. Abakumov

G.A. Razuvaev Institute of Organometallic Chemistry, Russian Academy of Sciences, 49 Tropinin Street, 603950 Nizhny Novgorod, Russia

Received July 16, 2010

The reaction of 8-quinolylhydrazine with 2 equiv of  $\text{Ph}_2\text{P}(\text{Cl})$  in the presence of  $\text{Et}_3\text{N}$  gives 8- $[(\text{Ph}_2\text{P})_2\text{NNH}]$ -Quin (**1**) (Quin = quinolyl) in 84% yield. The heating of **1** at 130 °C for 1 h in toluene results in migration of the  $[\text{Ph}_2\text{PNPPh}_2]$  group to a carbon atom of the quinolyl fragment to form an isomer, 7- $(\text{Ph}_2\text{P}-\text{N}=\text{PPh}_2)$ -8- $\text{NH}_2$ -Quin (**2**). The same migration is caused by the addition of  $\text{LiN}(\text{SiMe}_3)_2$  to **1**. On the contrary, lithiation of **1** with  $n\text{-BuLi}$  followed by the addition of  $\text{ZnI}_2$  (1:1) affords the aminoquinolyl–phosphazene dinuclear complex  $[\text{Zn}(\text{8-Quin-NPPh}_2=\text{N-PPh}_2)-\kappa^3\text{N,N,P}]_2$  (**4**), which is a result of P→N migration. Compound **1** itself reacts with  $\text{ZnI}_2$  in THF to form **4** and protonated molecule **1**·HI, which rearranges to the more stable iminobiphosphine salt  $(\text{Ph}_2\text{P}-\text{PPh}_2=\text{N-NH-Quin-8})\cdot\text{HI}$ . Zinc iodide reacts with 2 equiv of the lithium salt of **1** without rearrangement, to form homoleptic aminoquinolyl zinc complex  $\text{Zn}[\{(\text{Ph}_2\text{P})_2\text{NN-Quin-8}\}-\kappa^2\text{N,N}]_2$  (**6**). Solutions of **4** and **2** in dichloromethane show luminescence at 510 and 460 nm (quantum yields are 45% and 7%, respectively). DFT calculations were provided for possible isomers and their complexes.

### Introduction

Compounds bearing a phosphorus–nitrogen bond have attracted considerable attention both in heteroatom chemistry<sup>1</sup> and as ligands for transition metals as well.<sup>2</sup> A wide gradation in phosphorus–nitrogen bond energies attributed to the PN compounds of different types<sup>3</sup> is an important circumstance which makes possible template-like rearrangements and transformations of the phosphazene ligands in the coordination sphere of transition metals. Like the Michaelis–Arbuzov rearrangement<sup>4</sup>

and its modifications involving transition-metal centers,<sup>5</sup> the major driving force of these reactions is the formation of tetracoordinated phosphorus(V) species instead of P(III).

We have previously reported a migratory insertion of an  $\text{R}_2\text{P}$  group into the nitrogen–nitrogen bond of a phosphinohydrazide ligand, namely,  $\text{R}_2\text{P}-\text{NR}-\text{NR}- \rightarrow \text{RN}=\text{PR}_2-\text{NR}-$ , which in general occurred in the coordination sphere of s, d, and f metals.<sup>6–10</sup> This migration is a novel and useful approach to the synthesis of phosphazenes and phosphinoamides. Here, we discuss the unique properties of the diphosphinohydrazine **1** and diphosphinohydrazide ligand bearing a quinolyl substituent. Depending on the reaction conditions, these species demonstrate not only migration of

\*To whom correspondence should be addressed. E-mail: akornev@iomc.ras.ru.

(1) (a) Allcock, H. R. *Chem. Rev.* **1972**, *72*, 315–356. (b) Cowley, A. H.; Kemp, R. A. *Chem. Rev.* **1985**, *85*, 367–382. (c) Schmidpeter, A. *Heteroatom Chem.* **1999**, *10*(7), 529–537. (d) Stahl, L. *Coord. Chem. Rev.* **2000**, *210*, 203–250. (f) Nifantiev, E. E.; Grachev, M. K.; Burmistrov, S. Yu. *Chem. Rev.* **2000**, *100*, 3755–3799. (g) Bansal, R. K.; Heinicke, J. *Chem. Rev.* **2001**, *101*, 3549–3578. (h) Burford, N.; Conroy, K. D.; Landry, J. C.; Ragona, P. J.; Ferguson, M. J.; McDonald, R. *Inorg. Chem.* **2004**, *43*, 8245–8251.

(2) (a) Witt, M.; Roesky, H. W. *Chem. Rev.* **1994**, *94*, 1163–1181. (b) Bhattacharyya, P.; Woollins, J. D. *Polyhedron* **1995**, *14*(23–24), 3367–3388. (c) Ly, T. Q.; Woollins, J. D. *Coord. Chem. Rev.* **1998**, *176*, 451–481. (d) Appleby, T.; Woollins, J. D. *Coord. Chem. Rev.* **2002**, *235*, 121–140. (e) Richards, P. I.; Steiner, A. *Inorg. Chem.* **2004**, *43*, 2810–2817. (g) Fei, Z.; Dyson, P. J. *Coord. Chem. Rev.* **2005**, *249*, 2056–2074.

(3) (a) Corbridge, D. E. C. *Phosphorus. An Outline of its Chemistry Biochemistry and Technology*; Elsevier: Amsterdam, 1980. (b) Sudhakar, P. V.; Lammertsma, K. J. *Am. Chem. Soc.* **1991**, *113*(6), 1899–1906. (c) Steiner, A.; Zaccchini, S.; Richards, P. I. *Coord. Chem. Rev.* **2002**, *227*, 193–216.

(4) Bhattacharya, A. K.; Thyagarman, O. *Chem. Rev.* **1981**, *81*, 415–430.

(5) Brill, T. E.; Landon, S. J. *Chem. Rev.* **1984**, *84*, 577–585.

(6) Fedotova, Y. V.; Kornev, A. N.; Sushev, V. V.; Kurskiy, Yu. A.; Mushtina, T. G.; Makarenko, N. P.; Fukin, G. K.; Abakumov, G. A.; Zakharov, L. N.; Rheingold, A. L. *J. Organomet. Chem.* **2004**, *689*, 3060–3074.

(7) Sushev, V. V.; Kornev, A. N.; Min'ko, Y. A.; Belina, N. V.; Kurskiy, Yu. A.; Kuznetsova, O. V.; Fukin, G. K.; Baranov, E. V.; Cherkasov, V. K.; Abakumov, G. A. *J. Organomet. Chem.* **2006**, *691*, 879–889.

(8) Sushev, V. V.; Belina, N. V.; Fukin, G. K.; Kurskiy, Yu. A.; Kornev, A. N.; Abakumov, G. A. *Inorg. Chem.* **2008**, *47*, 2608–2612.

(9) Kornev, A. N.; Belina, N. V.; Sushev, V. V.; Fukin, G. K.; Baranov, E. V.; Kurskiy, Y. A.; Poddelskii, A. I.; Abakumov, G. A.; Lönnecke, P.; Hey-Hawkins, E. *Inorg. Chem.* **2009**, *48*, 5574–5583.

(10) Belina, N. V.; Kornev, A. N.; Sushev, V. V.; Fukin, G. K.; Baranov, E. V.; Abakumov, G. A. *J. Organomet. Chem.* **2010**, *695*, 637–641.

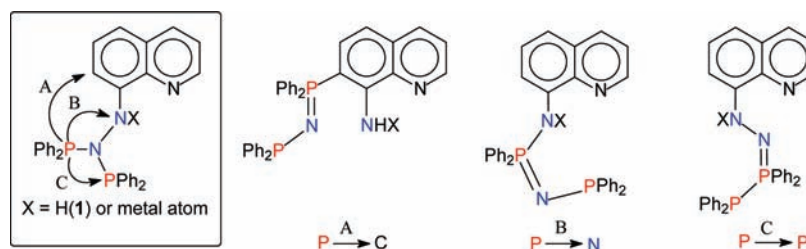
Scheme 1. Isomeric Transformations of **1** and Its Metal Derivatives

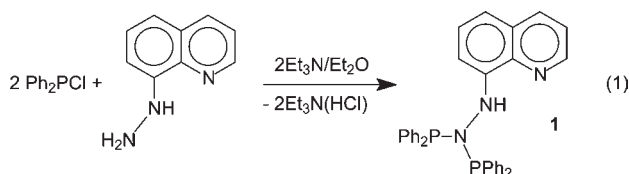
Table 1. Crystal and Structure Refinement

	1	2	4	6
empirical formula	C <sub>33</sub> H <sub>27</sub> N <sub>3</sub> P <sub>2</sub>	C <sub>33</sub> H <sub>27</sub> N <sub>3</sub> P <sub>2</sub>	C <sub>76</sub> H <sub>74</sub> I <sub>2</sub> N <sub>6</sub> OP <sub>4</sub> Zn <sub>2</sub>	C <sub>87</sub> H <sub>73</sub> N <sub>6</sub> P <sub>4</sub> Zn
fw	527.52	527.52	1595.83	1391.76
temp, K	100(2)	100(2)	100(2)	100(2)
cryst syst	monoclinic	triclinic	triclinic	triclinic
space group	<i>P</i> 2(1)/ <i>n</i>	<i>P</i> $\bar{1}$	<i>P</i> $\bar{1}$	<i>P</i> $\bar{1}$
unit cell dimensions				
<i>a</i> , Å	9.3768(4)	10.0674(5)	12.3881(5)	12.2550(16)
<i>b</i> , Å	28.0714(12)	11.7831(6)	12.4416(5)	17.405(2) Å
<i>c</i> , Å	10.5737(5)	12.5396(6)	12.9177(5)	17.594(2) Å
$\alpha$ , deg	90	96.9470(10)	107.3020(10)	80.360(3)
$\beta$ , deg	100.8010(10)	112.7310(10)	114.3250(10)	74.710(3)
$\gamma$ , deg	90	98.9730(10)	94.7250(10)	89.626(3)
volume, Å <sup>3</sup>	2733.9(2)	1328.10(11)	1683.41(12)	3566.0(8)
<i>Z</i>	4	2	1	2
density (calcd), Mg/m <sup>3</sup>	1.282	1.319	1.574	1.296
abs coeff, mm <sup>-1</sup>	0.187	0.192	1.776	0.486
cryst size, mm <sup>3</sup>	0.45 × 0.38 × 0.29	0.28 × 0.21 × 0.18	0.12 × 0.10 × 0.08	0.35 × 0.10 × 0.03
reflns collected	16973	8763	14357	28317
independent reflns	5638 [R(int) = 0.0158]	5765 [R(int) = 0.0224]	6553 [R(int) = 0.0241]	12511 [R(int) = 0.1671]
abs correction	semiempirical	semiempirical	semiempirical	semiempirical
	from equivalents	from equivalents	from equivalents	from equivalents
Max./min transm	0.9479/0.9207	0.9663/0.9482	0.8710/0.8152	0.9856/0.8483
refinement method	full-matrix	full-matrix	full-matrix	full-matrix
	least-squares on F <sup>2</sup>	least-squares on F <sup>2</sup>	least-squares on F <sup>2</sup>	least-squares on F <sup>2</sup>
data/restraints/params	5638/0/451	5765/0/351	6553/7/394	12511/3/793
R indices [ <i>I</i> > 2σ( <i>I</i> )]	R1 = 0.0350, wR2 = 0.0911	R1 = 0.0526, wR2 = 0.1281	R1 = 0.0413, wR2 = 0.1111	R1 = 0.0832, wR2 = 0.1297n
R indices (all data)	R1 = 0.0380, wR2 = 0.0929	R1 = 0.0719, wR2 = 0.1390	R1 = 0.0528, wR2 = 0.1169	R1 = 0.2119, wR2 = 0.1673
largest diff. peak and hole, e.Å <sup>-3</sup>	0.383 and -0.209	0.505 and -0.266	1.517 and -1.120	0.799 and -0.662

the Ph<sub>2</sub>P group into the N–N bond but also the migration of the [Ph<sub>2</sub>PNPPH<sub>2</sub>] fragment to the nearest carbon atom of the quinolyl substituent, and a reversible migration of the Ph<sub>2</sub>P group from nitrogen to the phosphorus atom of another Ph<sub>2</sub>P group (Scheme 1).

## Results and Discussion

2,2-Bis(diphenylphosphino)-1-(quinolyl-8)-hydrazine (**1**) was prepared by the reaction of 8-quinolylhydrazine with two equivalents of chlorodiphenylphosphine in the presence of Et<sub>3</sub>N (eq 1). It is a moisture- and air-resistant compound that is not decomposed below 100 °C.



The structure of **1** was determined by X-ray analysis (Supporting Information, Figure S1). Crystal data and some details of the data collection and refinement for **1** are given in Table 1.

The phosphorus and nitrogen atoms in the hydrazine fragment adopt an almost coplanar arrangement; the sum of the angles around N(1) is 356.7°. The N(1)–N(2) (1.418(1) Å) and P–N distances (1.723(1), 1.735(1) Å) are in the typical range found for diphenylphosphinohydrazines.<sup>6–10</sup> The <sup>31</sup>P{<sup>1</sup>H} NMR spectrum of **1** exhibits a single resonance at δ 70.7 ppm.

Heating of toluene or pyridine solutions of **1** under a vacuum at 130 °C for 1 h results in disappearance of this signal, while two doublets arose at 44.5 and 27.3 ppm. The observed coupling constant (*J*<sub>P,P</sub> = 104 Hz) is indicative of a new structure, containing phosphoranato and phosphino groups separated by the nitrogen atom. A strong and wide absorption band at 1150 cm<sup>-1</sup> in the IR spectrum is in accordance with the presence of the P=N–P chain. Further necessary information was obtained from an X-ray investigation indicating formation of the isomeric product **2** (eq 2).



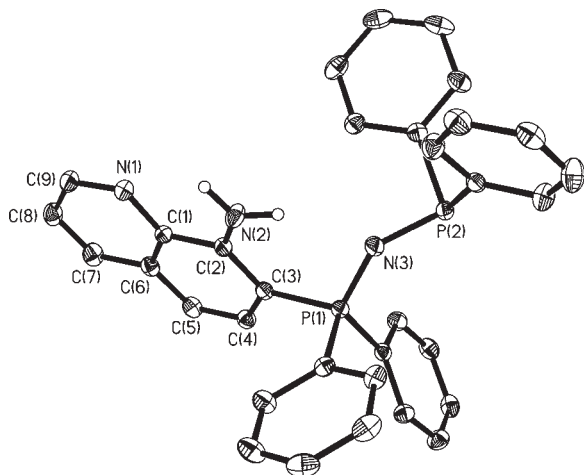


**Figure 1.** Molecular structure of **2**. Hydrogen atoms other than at N(2) are omitted for clarity. Ellipsoids are drawn at 30% probability. Selected bond lengths [Å] and angles [deg] for **2**: P(1)–N(3) 1.561(2), P(1)–C(3) 1.799(2), P(2)–N(3) 1.665(2), N(2)–C(2) 1.356(3), C(1)–C(6) 1.409(3), C(1)–C(2) 1.451(3), C(2)–C(3) 1.400(3); N(3)–P(1)–C(3) 111.3(1), P(1)–N(3)–P(2) 134.9(1), N(2)–C(2)–C(3) 123.8(2), N(2)–C(2)–C(1) 117.4(2).

Crystal data and some details of the data collection and refinement for **2** are given in Table 1.

The molecular structure of **2** (Figure 1) has two different P–N bonds: P(1)–N(3) = 1.561(2) Å of double bond character and P(2)–N(3) = 1.665(2) Å of single bond character. The P(1)–N(3)–P(2) angle of 134.9(1)° is in the range typical for iminophosphines.<sup>1a,11</sup> Inspection of the NBO partial charges in **1** (Supporting Information, Table S1) reveals that the greatest negative charge is localized on the carbon atom in position 7 of the quinolyl fragment, which makes it most favorable for electrophilic attack. It is reasonable to propose also that charge separation in the transition state (leading to the [Ph<sub>2</sub>P=N=PPh<sub>2</sub>]<sup>+</sup> cation and aminoquinolyl-anion) will promote the electrophilic substitution of the hydrogen atom, which migrates further to the amino-nitrogen to form **2** eventually.

Notably, the interaction of **1** with LiN(SiMe<sub>3</sub>)<sub>2</sub> in a toluene/ether solution at room temperature gave the lithium salt of the isomeric product **2** quantitatively. The <sup>31</sup>P NMR spectrum of the product contains two doublets at 41.7 and 22.7 ppm with a coupling constant of 115 Hz. Workup of this solution with water gave compound **2** according to the <sup>31</sup>P NMR and IR measurements.

Interestingly, *n*-BuLi did not cause rearrangement of **1**. The addition of one equivalent of *n*-BuLi to the toluene solution of **1** causes precipitation of the lithium salt **3**. The THF solution of **3** exhibits a single resonance in the <sup>31</sup>P{<sup>1</sup>H} NMR spectrum upfield shifted (61.3 ppm) when compared with the starting compound. The <sup>31</sup>P NMR monitoring of the solution indicated no dynamic processes during the next two weeks. In comparing these two reactions, it is evident that a dissociation equilibrium is possible in the reaction of **1** with LiN(SiMe<sub>3</sub>)<sub>2</sub>, while the reaction with *n*-BuLi is an irreversible process.

Lithium salt **3** reacts with zinc iodide to form different products depending on stoichiometry of the components. The equimolar mixture of ZnI<sub>2</sub> and **3** in THF was allowed to

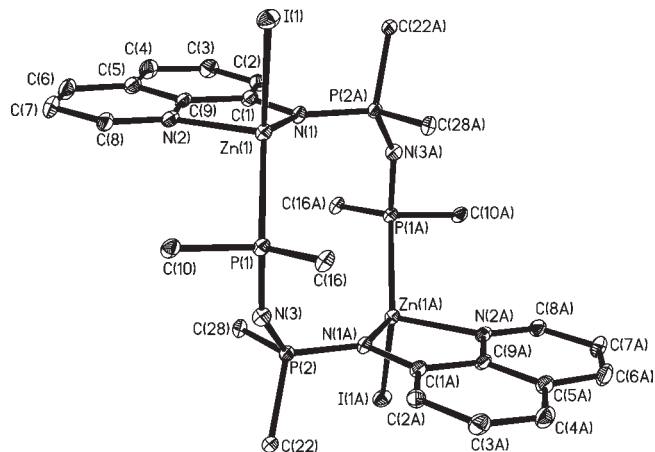
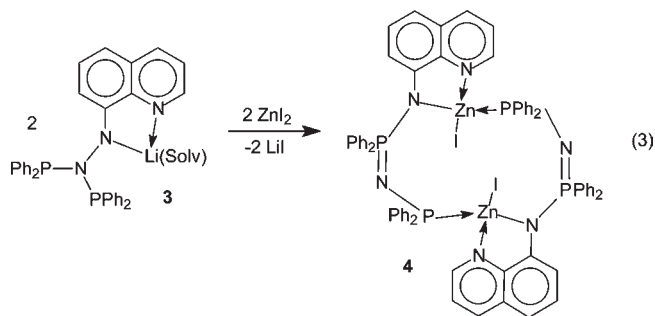


**Figure 2.** Molecular structure of [ZnI(8-Quin-NPPh<sub>2</sub>=N-PPh<sub>2</sub>)-κ<sup>3</sup>N,N,P]<sub>2</sub> (**4**). Hydrogen atoms and Ph rings at phosphorus atoms are omitted for clarity. Ellipsoids are drawn at 30% probability. Selected bond lengths [Å] and angles [deg] for **2**: Zn(1)–N(1) 1.987(2), Zn(1)–N(2) 2.079(2), Zn(1)–P(1) 2.3765(8), Zn(1)–I(1) 2.5920(4), P(1)–N(3) 1.609(3), P(2)–N(3) 1.560(3), P(2)–N(1A) 1.645(2); N(1)–Zn(1)–N(2) 83.19(9), N(1)–Zn(1)–P(1) 125.42(7), N(2)–Zn(1)–P(1) 107.50(7), N(1)–Zn(1)–I(1) 114.37(7), N(2)–Zn(1)–I(1) 102.01(7), P(1)–Zn(1)–I(1) 115.05(2), N(3)–P(1)–Zn(1) 123.2(1), P(2A)–N(1)–Zn(1) 127.8(1), N(3)–P(2)–N(1A) 119.0(1), P(2)–N(3)–P(1) 150.4(2).

react at room temperature for one week. Over this period of time, a yellow, crystalline precipitate formed.

X-ray analysis of these crystals clearly showed the formation of a binuclear zinc complex **4** bearing a novel isomeric ligand, which is a result of the migration and insertion of the Ph<sub>2</sub>P group into the nitrogen–nitrogen bond (Figure 2, eq 3).



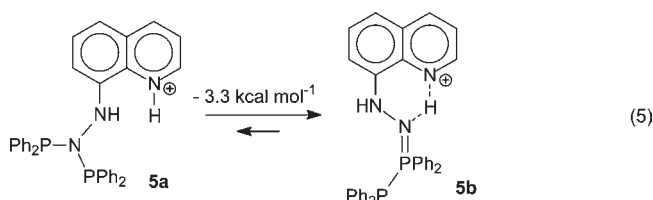
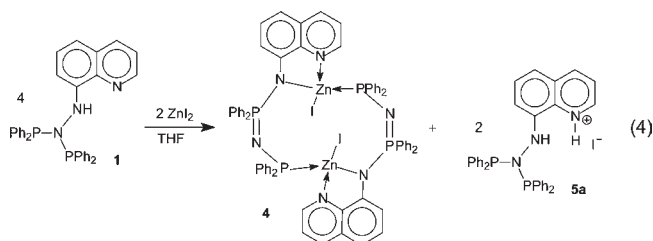
Both zinc atoms in the centrosymmetric dimer are surrounded in a distorted tetrahedral fashion by two nitrogen atoms of an aminoquinolyl group, one iodine atom, and one phosphorus atom from the adjacent ligand. So, two parts of the dimeric molecule are linked by normal coordination Zn–P bonds (2.3760(8) Å). Chair-like 10-membered metallocycle N<sub>4</sub>P<sub>4</sub>Zn<sub>2</sub> contains two short P=N bonds (1.560(3) Å) and four longer P–N bonds (two of 1.609(3) Å and two of 1.645(2) Å, that is typical for P–N single bonds). Notably, both aminoquinolyl ligand systems (including chelated zinc atoms) are coplanar; the distance between the planes is 4.514 Å, while the distance between Zn atoms is 5.77 Å. The amidonitrogen atoms (N(1), N(1A)) demonstrate trigonal planar geometry (sum of the angles of 359.51°). The imino-nitrogen atoms (N(3), N(3A)) have an internal P–N=P angle of 150.4(2)°, which is notably larger than usually found for similar compounds.<sup>11</sup> It may be due to the increased steric bulk of the dimeric unit. Chelated N–Zn–N angles (83.19(9)°) in this structure are within the normal range expected for the related complexes.<sup>12</sup> Compound **4** crystallized

(11) Lewis, G. R.; Dance, I. J. *Chem. Soc., Dalton Trans.* **2000**, 299–306.

in the  $P\bar{1}$  space group with one equivalent of solvates  $\text{Et}_2\text{O}$  and *c*-hexane as part of the crystal lattice.

Complex **4** is a reasonably air-stable, crystalline solid that can be handled in the open laboratory for short periods of time. The  $^{31}\text{P}\{^1\text{H}\}$  NMR spectrum of **4** contains two resonances at 23.8 ( $\text{P}^{\text{III}}$ ) and 3.5 ( $\text{P}^{\text{V}}$ ) ppm, but the  $^2J_{\text{P-P}}$  coupling constant could not be resolved. The NBO charges of these phosphorus atoms are +1.17 *e* and +2.13 *e*, respectively. Such a large difference in charges is explained by the distinction between the  $\text{P}^{\text{III}}$  and  $\text{P}^{\text{V}}$  valent states. The natural charge on the nitrogen atom of the P–N–Zn fragment is smaller than that of the atom belonging to the P–N–P group, but the difference is not so large (–1.17 *e* and –1.49 *e*, respectively).

It was found that dimer **4** may be synthesized in another way, by the direct interaction of  $\text{ZnI}_2$  with diphosphino-hydrazine **1**. In this case, quinoline derivative **1** may provide a HI abstraction (eq 4).  $^{31}\text{P}\{^1\text{H}\}$  NMR monitoring of this reaction revealed the formation of **4** (two singlets at 23.8 and 3.5 ppm), and a new product, showing two doublets at 49.4 and –19.5 ppm. Large coupling constant ( $J_{\text{P,P}} = 266$  Hz) allowed us to propose the formation of a molecule, containing an iminobiphosphine fragment. It is known that the protonation of diphosphinoamines attached to pyridine at the ortho position quantitatively affords the corresponding iminobiphosphine isomers.<sup>13</sup> In our case, the formation of proton-stabilized unit **5b** (eqs 4 and 5) is energetically more favorable by 3.3 kcal/mol than its isomer **5a** according to the DFT calculation (Supporting Information, Table S2).



It is reasonable to propose that reactions 3 and 4 may give mononuclear zinc complex together with the dimer **4**. However, we could not detect or isolate the monomeric species. DFT calculations showed that the dimerization process is energetically favorable by 11.7 kcal (Supporting Information, Table S3). Moreover, the formation of **4** may be a result of low solubility of this compound.

(12) Malassa, A.; Koch, C.; Stein-Schaller, B.; Gorls, H.; Friedrich, M.; Westerhausen, M. *Inorg. Chim. Acta* **2008**, *361*(5), 1405–1414.

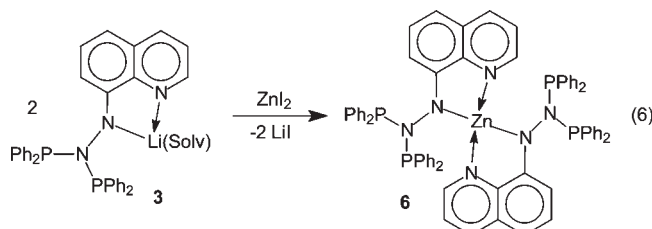
(13) Fei, Z.; Biricik, N.; Zhao, D.; Scopelliti, R.; Dyson, P. J. *Inorg. Chem.* **2004**, *43*, 2228–2230.

(14) So, the lithium bisphosphino-hydrazide,  $i\text{Pr}_2\text{P-NMe-NLi-PiPr}_2$ , was found to rearrange immediately under preparation in a THF solution into iminophosphoranate  $\text{LiN}=\text{PiPr}_2\text{-NMe-PiPr}_2$ . At the same time, quite stable *ate*-complex  $\text{Li}(\text{DME})_3[\text{Li}\{(\text{NPh-NPh-PiPr}_2)\text{-}\kappa\text{N}\}_2]$  shows a strongly elongated N–N bond compared to that of the starting compound,  $\text{HNPh-NPh-PiPr}_2$ .

Recently, we have shown<sup>9</sup> that the main factor, which controls the P–N–N to N=P–N rearrangement, is the charge at the hydrazido nitrogen. A strong negative charge promotes elongation of the N–N bond and/or its cleavage.<sup>14</sup> It is obvious that the mechanism of this rearrangement will be different for alkaline and late transition metals since the last ones usually have a strong P→M coordination bond together with back-donation. It takes additional energy to destroy this bond.<sup>15</sup> Formation of the zinc dimer **4** requires about a week. Tentatively, this reaction has two steps as minima. The first is the N–N bond cleavage; the second step involves coupling of the remaining particles in the zinc coordination sphere by the novel P–N bond formation.

The reaction of  $\text{ZnI}_2$  with 2 equiv of **3** produced the iodine-free homoleptic compound **6** (eq 6).

Notably, that the color of the reaction mixture in this case turned dark within a few hours.



Following removal of the solvent under a vacuum, extraction of the product with benzene, and crystallization at 10 °C, affords dark-red crystals of **6** suitable for X-ray analysis. The X-ray structure determination of **6** reveals the formation of the bis(amidoquinolyl) zinc complex having distorted tetrahedral geometry (Figure 3). The rigid aminoquinolyl framework of **6** prevents intramolecular coordination P→Zn. The Zn–P distances are in the range of 4.040–4.154 Å.

The N–N bonds in **6** (1.435(5) and 1.436(5) Å) are *ca.* 0.02 Å longer than that in the starting compound **1**. This is a small elongation when compared to the known zinc hydrazide,  $[\text{EtZn}(\text{NHNMe}_2)]_4$ , where the N–N bond distances are in the range of 1.447–1.464 Å.<sup>16</sup> The P–N bond distances in **6** are slightly different (1.739(4), 1.703(4), 1.731(4), and 1.714(4) Å) and comparable to those within the starting ligand. Compound **6** (and **3** as well) does not undergo further rearrangement. Apparently, this is due to delocalization of the negative charge of the hydrazido nitrogen over the five-membered metallocycle and quinoline rings, which prevents the N–N bond cleavage.

The  $^{31}\text{P}$  NMR spectrum of **6** demonstrates the equivalence of all phosphorus atoms at room temperature in THF solution, showing a single resonance at 43.5 ppm. The crab-like structure of **6** has large chelate arms. The distance between the phosphorus atoms of the different arms (P1 and P3) is 4.93 Å. This value is quite suitable for heterobimetallic complex formation with metals of the fifth and sixth periods.

Solutions of **2** and **4** in methylene chloride or acetonitrile glow yellow-green under visible light. Figure 4 demonstrates emission of the solution of **4** in  $\text{CH}_2\text{Cl}_2$  at 510 nm when excited by 450 nm light. An excitation band at 380 nm is observed upon monitoring the emission at 510 nm. The electronic absorption spectrum of this complex also shows a peak at 380 nm, the experimental transition energy (3.26 eV)

(15) Rearrangements of the Ni and Co phosphino-hydrazides usually take 1–2 days at ambient conditions.

(16) Redshaw, C.; Elsegood, M. R. J. *Chem. Commun.* **2006**, 523–525.

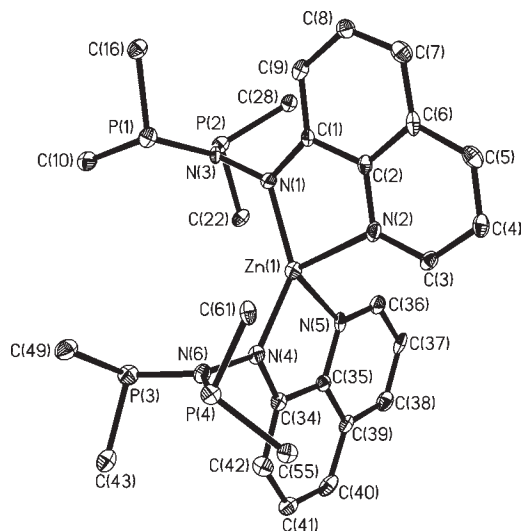


**Figure 3.** Molecular structure of  $\text{Zn}[(\text{Ph}_2\text{P})_2\text{NN-Quin-8}-\kappa^2\text{N,N}]_2$  (**6**). Hydrogen atoms and Ph rings at phosphorus atoms are omitted for clarity. Ellipsoids are drawn at 30% probability. Selected bond lengths [Å] and angles [deg] for **6**: N(1)–N(3) 1.436(5), N(4)–N(6) 1.435(5), Zn(1)–N(4) 1.954(4), Zn(1)–N(1) 1.961(4), Zn(1)–N(5) 2.077(4), Zn(1)–N(2) 2.083(4), P(1)–N(3) 1.739(4), P(2)–N(3) 1.703(4), P(3)–N(6) 1.731(4), P(4)–N(6) 1.714(4); N(4)–Zn(1)–N(1) 139.7(2), N(4)–Zn(1)–N(5) 83.0(2), N(1)–Zn(1)–N(5) 128.3(2), N(4)–Zn(1)–N(2) 121.5(2), N(1)–Zn(1)–N(2) 82.2(2), N(5)–Zn(1)–N(2) 99.0(2), N(1)–N(3)–P(2) 119.8(3), N(1)–N(3)–P(1) 115.2(3), P(2)–N(3)–P(1) 125.0(2), N(4)–N(6)–P(4) 122.0(3), N(4)–N(6)–P(3) 114.9(3), P(4)–N(6)–P(3) 123.1(2).

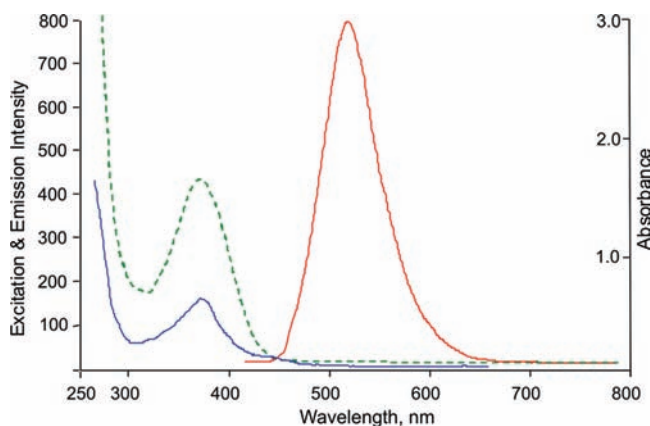


**Figure 4.** Electronic absorption (dotted green), emission (red), and excitation (blue) (monitored at 510 nm) spectra of **4** in  $\text{CH}_2\text{Cl}_2$  at 298 °C.

agreeing well with the calculated HOMO–LUMO gap (3.48 eV). The distribution of the electron density corresponding to the HOMO and LUMO (Supporting Information, Figure S2) suggests that the transition observed is associated with the electron density transfer from the iodine atoms and the nitrogen atoms of the 10-membered metallacycle to the quinoline fragment. The quantum yield of luminescence calculated relative to rhodamine 6G is 45%. It is worth mentioning that the mononuclear zinc complex **6** demonstrates no emission both in the solid state and in solution, while the spectral properties of **2** are similar to those of 8-aminoquinoline: maxima of excitation and emission are observed at 370 and 460 nm, respectively, in  $\text{CH}_2\text{Cl}_2$  solution (Supporting Information, Figure S3); however, the quantum yield of luminescence is much lower (7%).

## Experimental Session

**General Remarks.** Solvents were purified following standard methods.<sup>17</sup> Toluene and *c*-hexane were thoroughly dried and distilled over sodium prior to use. Diethyl ether and THF were dried and distilled over Na/benzophenone. 8-Quinolylhydrazine was synthesized according to a known method.<sup>18</sup>

Chlorodiphenylphosphine and zinc iodide were purchased from Sigma-Aldrich Chemical Co. and used as received. All manipulations were performed in a vacuum or under an argon atmosphere using standard Schlenk techniques. NMR spectra were recorded in  $\text{CDCl}_3$  or  $\text{C}_6\text{D}_6$  solutions using a Bruker DPX-200 spectrometer. Absorption and photoluminescence spectra of **2** and **4** were recorded on a Perkin-Elmer Lambda UV–vis spectrometer at 25 °C. Infrared spectra were recorded on a Perkin-Elmer 577 spectrometer from 4000 to 400  $\text{cm}^{-1}$  in nujol or on a Perkin-Elmer FT-IR Spectrometer System 2000 as KBr mulls.

**Computational Details.** DFT calculations performed in this work were carried out at the B3LYP/6-31G(d) level of theory with the Gaussian 03 package (supporting general information). The optimized geometries of the compounds **1**, **2**, **4**, **5a**, **5b**, and **6** correspond to energy minima, as indicated by frequency computations. For the geometry optimization of **1**, **2**, **4**, and **6**, we used the full structure without simplification and the B3LYP/6-31G(d) level of theory. The structure corresponds to an energy minimum.

**X-Ray Crystallography.** The X-ray diffraction data of **1**, **2**, **4**, and **6** were collected on a SMART APEX diffractometer (graphite-monochromated, Mo  $\text{K}\alpha$  radiation,  $\varphi$ - $\omega$ -scan technique,  $\lambda = 0.71073$  Å). The intensity data were integrated by the SAINT program.<sup>19</sup> SADABS<sup>20</sup> was used to perform area-detector scaling and absorption corrections. The structures were solved by direct methods and were refined on  $F^2$  using all reflections with the SHELXTL package.<sup>21</sup> All non-hydrogen atoms were refined anisotropically. All H atoms in **1** were found from Fourier syntheses of electron density and were refined isotropically, whereas in **2**, **4**, and **6** they are located in calculation positions and were refined isotropically in the rigid model. Details of crystallographic, collection, and refinement data for all compounds are shown in the Table 1.

CCDC 780260 (**1**), 780261 (**2**), 780262 (**4**), and 780263 (**6**) contain the supplementary crystallographic data for this paper. These data can be obtained free of charge at [www.ccdc.cam.ac.uk/const/retrieving.html](http://www.ccdc.cam.ac.uk/const/retrieving.html) from the Cambridge Crystallographic Data Centre, 12 Union Road, Cambridge CB2 1EZ, U.K.; fax: (internat.) +44–1223/336–033; e-mail: [deposit@ccdc.cam.ac.uk](mailto:deposit@ccdc.cam.ac.uk).

**Synthesis.** **2,2-(Diphenylphino)-1-(quinolyl-8)-hydrazine (1) and Its Lithium Salt (3).** A solution of chlorodiphenylphosphine (4.41 g, 20.0 mmol) in 20.0 mL of THF was added dropwise to a mixture of 8-quinolylhydrazine (1.59 g, 10.0 mmol) and  $\text{Et}_3\text{N}$  (2.53 g, 25.0 mmol) in the same solvent. The mixture was stirred for 24 h at 20 °C and then filtered. The solvent was removed in a vacuum and replaced with toluene. Next, the solution was concentrated to 10.0 mL. Keeping the mixture overnight at 10 °C yielded large pale yellow crystals of **1**. Yield: 4.96 g (94%). Anal. calcd for  $\text{C}_{33}\text{H}_{27}\text{N}_3\text{P}_2$ , %: C, 75.13; H, 5.16; P, 11.74. Found, %: C, 75.20; H, 5.11; P, 11.70.  $^1\text{H}$  NMR ( $\text{CDCl}_3$ , 300 K)  $\delta$  (ppm): 8.63 (dd, 1H,  $^3J_{\text{HH}} = 4.0$  Hz,  $^4J_{\text{HH}} = 1.8$  Hz), 7.98 (dd, 1H,  $^3J_{\text{HH}} = 8.3$ ,  $^4J_{\text{HH}} = 1.8$  Hz); 6.4–7.8 (m, 24H, Ph and quinolyl protons), 8.33 (s, broad, 1H, NH).  $^{31}\text{P}\{^1\text{H}\}$  NMR

(17) Perrin, D. D.; Armarego, W. L. F.; Perrin, D. R. *Purification of Laboratory Chemicals*; Pergamon: Oxford, 1980.

(18) (a) Dewar, M. J. S. *J. Chem. Soc.* **1944**, 615–619. (b) Krasavin, I. A.; Parusnikov, B. V.; Dziomko, V. M. 8-Quinolylhydrazine and its hydrochloride. In *Preparation of chemical reagents (In Russian)*; Moscow, 1963; Vol. 7, pp 5–7.

(19) *SAINTPlus Data Reduction and Correction Program*, v. 6.02a; Bruker AXS: Madison, WI, 2000.

(20) Sheldrick, G. M. *SADABS*, v.2.01; Bruker AXS: Madison, WI, 1998.

(21) Sheldrick, G. M. *SHELXTL*, v. 6.12; Bruker AXS: Madison, WI, 2000.

(CDCl<sub>3</sub>, 300 K),  $\delta$  (ppm): 70.7. IR (nujol),  $\nu/\text{cm}^{-1}$ : 3295w, 1577m, 1505m, 1112s broad, 900m, 882w, 817m, 794w, 741s, 694s, 670w, 638w, 616w, 600w, 535w, 493m.

The lithium salt of **1**, viz. **3**, was prepared by the addition of an equivalent of *n*-BuLi (1.0 M solution in hexane) to a toluene solution of **1**. Orange crystals of the lithium salt **3** formed quickly were filtered and dissolved in THF. <sup>31</sup>P{<sup>1</sup>H} NMR (THF, 300 K):  $\delta$  61.3 ppm.

**Thermal Rearrangement of 1.** A solution of **1** (1.00 g) in toluene (10 mL) was heated under a vacuum for 1 h at 130 °C. The resulting solution was cooled to room temperature and then kept overnight at 0 °C. Pale yellow crystals of **2** were filtered and dried in a vacuum. Yield: 0.90 g (90%). Anal. Calcd for C<sub>33</sub>H<sub>27</sub>N<sub>3</sub>P<sub>2</sub>, %: C, 75.13; H, 5.16; P, 11.74. Found, %: C, 75.08; H, 5.19; P, 11.67. <sup>1</sup>H NMR (CDCl<sub>3</sub>, 300 K)  $\delta$  (ppm): 8.76 (dd, 1H, <sup>3</sup>J<sub>HH</sub> = 4.2 Hz, <sup>4</sup>J<sub>HH</sub> = 1.7 Hz; 8.00 (dd, 1H, <sup>3</sup>J<sub>HH</sub> = 8.3 Hz, <sup>4</sup>J<sub>HH</sub> = 1.7 Hz); 7.9–6.8 (m, 25H, Ph, quinolyl and NH<sub>2</sub> protons). <sup>31</sup>P{<sup>1</sup>H} NMR (CDCl<sub>3</sub>, 300 K),  $\delta$  (ppm): 44.5 (d, J<sub>P,P</sub> = 104 Hz), 27.3 (d, J<sub>P,P</sub> = 104 Hz). Note, **2** reacts with CDCl<sub>3</sub> for a few days to give a mixture of products. IR (nujol),  $\nu/\text{cm}^{-1}$ : 3435m, 3226m (NH<sub>2</sub>), 1601w, 1577m, 1150 (P=N–P, s, wide), 1107sh, 1026w, 997w, 861w, 825m, 797w, 733sh, 720s, 695s, 635m, 534m.

**Interaction of 1 with (Me<sub>3</sub>Si)<sub>2</sub>NLi in a Ratio of 1:1.** A solution of (Me<sub>3</sub>Si)<sub>2</sub>NLi (0.50 g, 3.0 mmol) in 10 mL of toluene was added to a solution of **1** (1.58 g, 3.0 mmol) in 10 mL of the same solvent. After the mixture was kept at room temperature for 3 h, 0.5 mL of Et<sub>2</sub>O was charged into the system *via* syringe, and the crystallization was initiated. The mixture was left undisturbed for a few hours, and bright yellow crystals formed. <sup>31</sup>P{<sup>1</sup>H} NMR (THF, 300 K),  $\delta$  (ppm): 41.7 (d, J<sub>P,P</sub> = 115 Hz), 22.7 (d, J<sub>P,P</sub> = 115 Hz). IR (nujol),  $\nu/\text{cm}^{-1}$ : 3438w, 3333w, 1583 m, 1530 m, 1496 m, 1400 m, 1300 m, 1260 m, 1240 m, 1110s, 1060s, 870 m, 800 m, 740s, 695s, 645 m. Note that using THF in this reaction is not possible since the equilibrium in this case is shifted to the red lithium salt **3**.

**Interaction of 3 with ZnI<sub>2</sub> in a Ratio of 1:1.** A solution of ZnI<sub>2</sub> (0.67 g, 2.1 mmol) in 10 mL of THF was added to a solution of **3** (2.0 mmol, prepared from 1.05 g of **1** and 2.0 mL of 1.0 M *n*-BuLi) in 15 mL of the same solvent at –20 °C. The reaction mixture was stirred for 6 h and then concentrated to 10 mL. Allowing the mixture to set at room temperature for a week afforded the product as yellow fine crystals. Yield: 0.72 g (50%). Anal. Calcd for C<sub>66</sub>H<sub>52</sub>I<sub>2</sub>N<sub>6</sub>P<sub>4</sub>Zn<sub>2</sub> (**4**): C, 55.14; H, 3.65; I, 17.65; N, 5.85. Found, %: C, 55.20; H, 3.69; N, 5.93. <sup>31</sup>P{<sup>1</sup>H} NMR (CH<sub>2</sub>Cl<sub>2</sub>), 300 K),  $\delta$  (ppm): 23.8 (s), 3.5 (s). IR (nujol),  $\nu/\text{cm}^{-1}$ : 1576w, 1500w, 1313m, 1297m, 1260s, 1192w, 1131s, 963m, 870m, 822m, 777m, 746m, 697m, 548m, 530m. Single crystals

of **4** suitable for X-ray diffraction were grown from the mixture of solvents: CH<sub>2</sub>Cl<sub>2</sub>/Et<sub>2</sub>O/C<sub>6</sub>H<sub>12</sub> in a ratio of 3:1:1 respectively.

**Interaction of 3 with ZnI<sub>2</sub> in a Ratio of 2:1.** A solution of ZnI<sub>2</sub> (0.64 g, 2.0 mmol) in 10 mL of THF was added to a solution of **3** (2.11 g, 4.0 mmol) in 20 mL of the same solvent. The solution was stirred at room temperature for 3 h, over which time the solution turned dark red. Following removal of the solvent under a vacuum, the product was extracted with benzene, and the resulting solution was concentrated until crystalline material began precipitating. The solution was cooled to 10 °C, resulting in the formation of dark-red crystals (2.20 g, 79% yield). Anal. Calcd for C<sub>66</sub>H<sub>52</sub>N<sub>6</sub>P<sub>4</sub>Zn(C<sub>6</sub>H<sub>6</sub>)<sub>3.5</sub> (**6**), %: C, 75.08; H, 5.29; N, 6.04. Found, %: C, 74.97; H, 5.33; N, 5.95. <sup>31</sup>P{<sup>1</sup>H} NMR (THF, 300 K),  $\delta$  (ppm): 71.1 (s, broad). IR (nujol),  $\nu/\text{cm}^{-1}$ : 1571m, 1324m, 1278w, 1232w, 1180w, 1150w, 1114w, 1090m, 1020m, 899s, 816m, 795m, 741s, 698s, 680s, 496m.

## Conclusion

In summary, we report the unique properties of diphosphinohydrazide ligand (**1**) bearing an 8-quinolyl substituent, which demonstrates three types of isomeric transformations. These are (1) migration of the [Ph<sub>2</sub>PNPPH<sub>2</sub>] block to the nearest carbon atom of the quinolyl fragment under heating or under the action of LiN(SiMe<sub>3</sub>)<sub>2</sub>, (2) migration of the Ph<sub>2</sub>P group to another one to form iminodiphosphine upon protonation of **1**, and (3) migration and insertion of a Ph<sub>2</sub>P group into the N–N bond proceeding in the Zn(II) coordination sphere. The last transformation gave binuclear zinc complex **4** eventually, which shows strong electronic emission in CH<sub>2</sub>Cl<sub>2</sub> solution at 510 nm ( $\phi = 0.45$ ). Compound **2** may be considered as a new ligand, bearing two chelate rings of different functionality, that may be useful for the design of heterobimetallic complexes.

**Acknowledgment.** This work was supported by The Russian President's program "Leading Scientific Schools" (No. 4182.2008.3). We thank Dr. O. V. Kouznetsova and N. M. Khamaletdinova for IR measurements.

**Supporting Information Available:** Crystallographic information for **1**, **2**, **4**, and **6** in CIF format; molecular structure, selected bond lengths and angles, and NBO charges for **1**; HOMO and LUMO view for **4**; electronic emission and excitation spectra of **2**; and B3LYP calculated structures of the protonated molecules **5a** and **5b**. This material is available free of charge via the Internet at <http://pubs.acs.org>.